Mar 11th - Mar 15th

# Analysis of Site Effects at the Garner Valley Downhole Array Near the San Jacinto Fault

Sandra H. Seale
*Institute for Crustal Studies, Santa Barbara, California*

Ralph J. Archuleta
*University of California, Santa Barbara, California*

Proceedings: Second International Conference on Recent Advances in Geotechnical Earthquake Engineering and Soil Dynamics, March 11-15, 1991, St. Louis, Missouri, Paper No. 8.13

# Analysis of Site Effects at the Garner Valley Downhole Array Near the San Jacinto Fault

**Sandra H. Seale**
Assistant Research Geophysicist, Institute for Crustal Studies, Santa Barbara, California, USA

**Ralph J. Archuleta**
Professor of Seismology, Department of Geological Sciences, University of California, Santa Barbara, California, USA

SYNOPSIS: The Garner Valley downhole array is located in the geologically complicated and seismologically active San Jacinto fault zone. The choice of the site and the potential for a large earthquake there are discussed. The equipment is described in detail. The data recorded through the end of 1 April 1990 are summarized. Two large events at different locations are discussed in some detail and analyzed for amplification of the signal at the surface.

## INTRODUCTION

The San Jacinto fault zone in southern California is geologically complicated and seismologically very active (Figure 1). In the 250-km-long fault zone, Sanders (1989) identified twenty principal segments with lengths from 7 km to 35 km. Fletcher *et al.* (1987) identified a 40-km-long section of the San Jacinto fault zone around the town of Anza as a seismic gap. The 40 km of the San Jacinto fault zone between the intersection of the Banning fault and the northern end of the Anza seismic gap is a zone that has not ruptured since 1899 or 1918. Sykes and Nishenko (1984) calculated conditional probabilities that segments of the San Jacinto fault will be the site of a large earthquake in a 20 year period. They assigned the zone from Cajon Pass to Riverside a probability of 97-100%, at Riverside 6-64%, from Riverside to Anza 1-34%, and from Anza to Coyote Mountain 4-86%. Rockwell *et al.* (1990) computed a slip deficit of 0.8 m since the 1918 event and 1.1 m since the 1899 event for the 20-km-long segment north of Anza. The authors concluded that ". . . the Anza section of the fault is capable of producing a near future earthquake in the range of M6.5 - M 7."

In selecting a site for a downhole array of accelerometers, we chose a location near the Anza seismic gap. Fletcher *et al.* (1987) pointed out that there is a high rate of seismicity around the Anza seismic gap. Sanders (1989) identified clusters of seismicity at the intersection of the Banning fault and along the northwest Anza and southeast Hot Springs segments. The Garner Valley downhole array (GVDA) is located at Lake Hemet, at the southern end of the Hot Springs segment of the San Jacinto fault zone and the northern end of the Anza seismic gap (Figure 2). In this location, we are able to record the background seismicity as well as large events. An increase in the rate of background seismicity could be a precursor to a large event. Thus, our site is well chosen for monitoring the Anza seismic gap.

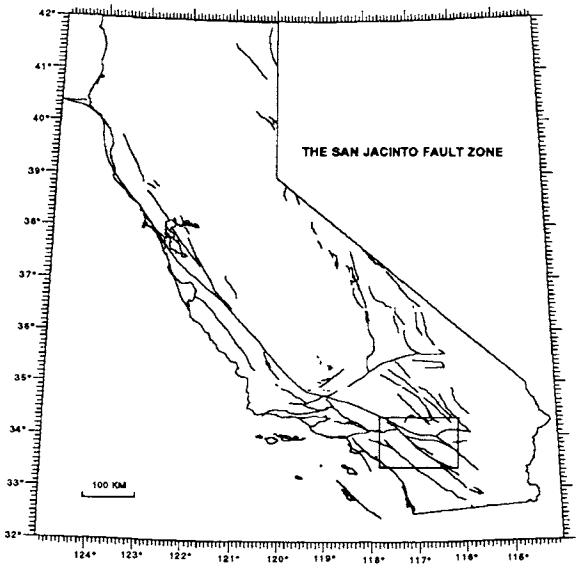


Figure 1. A map of California, the box shows the San Jacinto fault zone branching off the San Andreas and continuing to the south.

## INSTRUMENTATION

The downhole array consists of five, 3-component, dual-gain, feedback accelerometers (FBA) (Sangas *et al.* (1989), Archuleta and Seale (1989), Archuleta and Sangas (1989)). In a 3m x 3m area, there is a surface instrument at the center and boreholes were drilled to depths of 6 m, 15 m, 22 m and 220 m (Figure 3). The accelerometers are Kinemetrics FBA-13DH which were modified to provide dual outputs (high-gain and low-gain) for each component. The high-gain response to acceleration is uniform from 0.025 - 100 Hz; the low-gain is uniform from DC to 100 Hz. By recording the low- and high-gain output of each component simultaneously using a 16-bit (90 dB dynamic range) Tustin A/D, we take advantage of the FBA's full dynamic range of 120 dB. We can record on-scale accelerations from 2.0 x $10^{-6}$ g to 2.0 g with a 64 dB overlap between the high- and low-gain channels. The output of each instrument is digitized by the A/D at 500 samples/sec and lowpassed using 6-pole antialias filters with a corner frequency of 100 Hz. Absolute time is inserted into the data stream from a GOES satellite receiver. The recorders have 5 seconds of pre-event memory for the recovery of the first-arriving compressional waves. The digital data are read into a DEC MicroVAX II data logger that has been programmed with a STA/LTA triggering algorithm to determine if an event has been recorded. The on-site recording equipment has AC power and an UPS backup source.

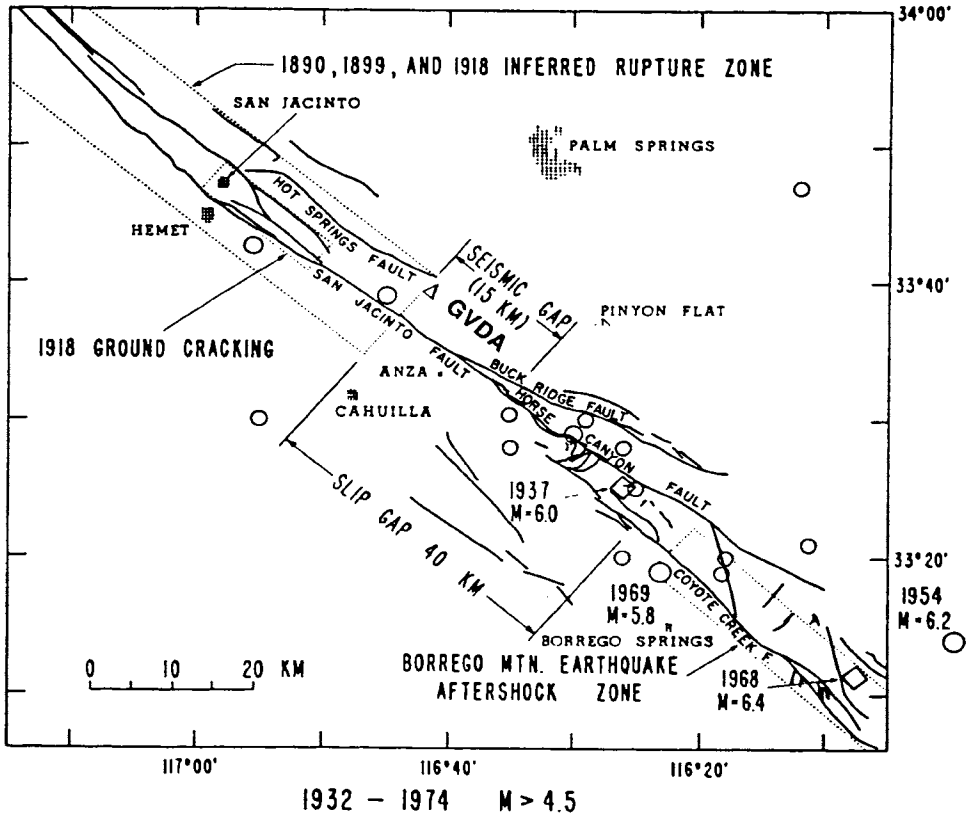


Figure 2. A geographical map of the area around the Garner Valley downhole array (Δ GVDA), showing the major faults, locations c historical seismicity and epicenters for earthquakes with M>4.5 recorded from 1932 to 1974 (from Fletcher *et al.* (1987)).

## DATA

### Introduction

Data from the Garner Valley downhole array can give a detailed description of the effects that the soil column has on the propagation of seismic waves. An instrument is placed in the basement rock for reference; three are located in the soil column and one is at the surface. Although outside the scope of this paper, particular attention is focussed on the seismic waves as they enter or exit material boundaries. With the bandwidth and the dynamic range of the instruments, the complete spectra of amplitudes of seismic waves can be directly compared.

### Velocity Profile

The surface material at the site is soil, to a depth of 20 m. Below the soil a layer of weathered granite extends to a depth of 42 m. The basement rock is granite. The boreholes at GVDA were logged for P- and S-wave velocities. Details of this work are described by Gibbs (1989). S waves and P waves were generated and recorded at 5 m intervals with a geophone inside a cased borehole. The travel time plots of P- and S-wave picks are fit with straight line segments to determine the velocities. The resulting velocities and the soil profile are shown in Figure 4. The near-surface P-wave velocity of 400 m/sec is not well constrained and is probably incorrect, since the velocity of sound in air is 332 m/sec.

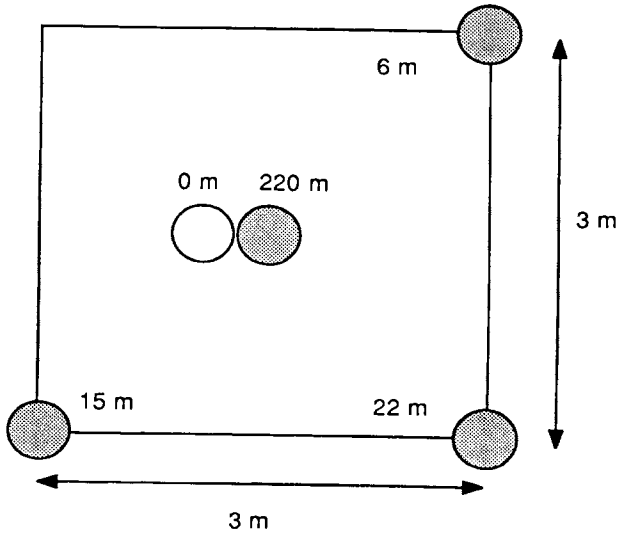


Figure 3. Plan view of accelerometer locations and depths.

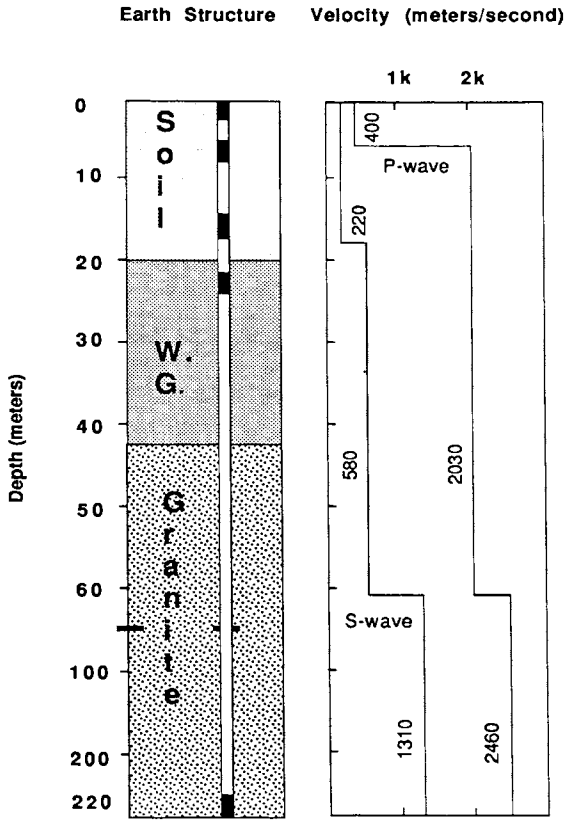


Figure 4. The soil profile and P- and S-wave velocities at the GVDA site. The first 20 m are soil, overlying weathered granite to 42 m. The basement rock is granite (Gibbs (1989)).

## Earthquakes

Operation of the array began 14 July 1989 with intermittent power failures. After installation of the UPS, full operation commenced 16 August 1989. From July 1989 through April 1990, GVDA has recorded 130 events with magnitudes from 1.4 to 4.7. December 1989 was a particularly active month, with 39 earthquakes of $M \geq 1.4$. All events recorded from July through December 1989 are shown in Figure 5.

In December 1989 a cluster of events occurred 8-9 km from the site. The largest was a M 4.2 earthquake on 2 December 1989 at an epicentral distance of 8.2 km and depth of 14.5 km. The uphole and downhole acceleration records are shown in Figure 6a and 6b. The peak acceleration at 220 m is 30.2 cm/sec$^2$ on the vertical component; at the surface it is 87.6 cm/sec$^2$ on the vertical component.

Two large aftershocks of the Upland's earthquake (28 February 1990, M 5.5) were recorded at GVDA. The first was on 1 March 1990, M 4.7, at an epicentral distance 110 km. The uphole and downhole acceleration records are shown in Figure 7a and 7b. The peak acceleration at 220 m is 0.482 cm/sec$^2$ on the second horizontal component; at the surface it is 2.048 cm/sec$^2$ on the same component.

## ANALYSIS

The two events shown in Figures 6 and 7 were analyzed to determine the amplification of acceleration at the surface. For the December event, the amplifications of the peak acceleration of each component were 2.9, 2.9 and 2.2. We computed the Fast Fourier Transform (FFT) of the S wave with a window from t = 7.0 to 8.5 sec and a cosine half-bell taper at each end. We then divided the amplitude spectrum of the S wave at 0 m to that at 220 m. The spectral ratio of the second horizontal component is shown in Figure 8a. For the March event, the amplifications of the peak acceleration of each component were 3.0, 5.0 and 4.2. We computed the FFT of the S wave with a window from t = 17.0 to 24.0 sec and a cosine half-bell taper. The spectral ratio of the second horizontal component is shown in Figure 8b. The March spectral ratio shows a peak at 0.9 Hz. Both events show peaks around 9 Hz and 10.5 Hz. Above 10 Hz, the ratios drop off due to attenuation in the soil. Above 50 Hz, noise dominates the signal.

Earthquake source parameters were determined from the Fourier amplitude spectrum of displacements for 16 events recorded at GVDA with good signal-to-noise ratio (Archuleta and Sangas (1990)). A nonlinear fitting algorithm calculated corner frequency $f_c$, low-frequency asymptote LFA and quality factor Q for the displacement spectrum (out to 50 Hz) of the horizontal components of each event (Brune (1970)). For each component, the LFA was multiplied by the hypocentral distance R A plot of LFA x R at 220 m vs 0 m is shown in Figure 9. The best-fit line is drawn through these points. The intercept of the line ,12.8, represents the amplification of the amplitude spectrum in the lower frequencies ( < 5 Hz).

## CONCLUSIONS

The 2 December 1989 M 4.2 event generated a peak vertical acceleration at the surface that was twice the peak horizontal acceleration. Peak accelerations are amplified by a factor of 2.9. The 1 March 1990 M 4.7 event was 110 km away and therefore the accelerations have small amplitudes. The amplifications of the peak accelerations range from 3.0 to 5.0. Although these two events were 100 km apart, their S-wave spectral amplitudes show similar peaks at 9 and 10.5 Hz.

The low-frequency asymptotes of the horizontal displacement components of 16 events were calculated. The amplification of the displacements at the surface is represented by the intercept of the plot of LFA x R at 220 m vs 0 m. The intercept gave an amplification of 12.8 for frequencies < 5 Hz.

With more data, further work is planned to investigate the resonances of the soil and weathered granite layers. We will also take a closer look at the role of attenuation in the surface layers.

## ACKNOWLEDGMENTS

This research is supported by the Office of Nuclear Regulatory Research, U.S. Nuclear Regulatory Commission Grant No. NRC-04-88-146.

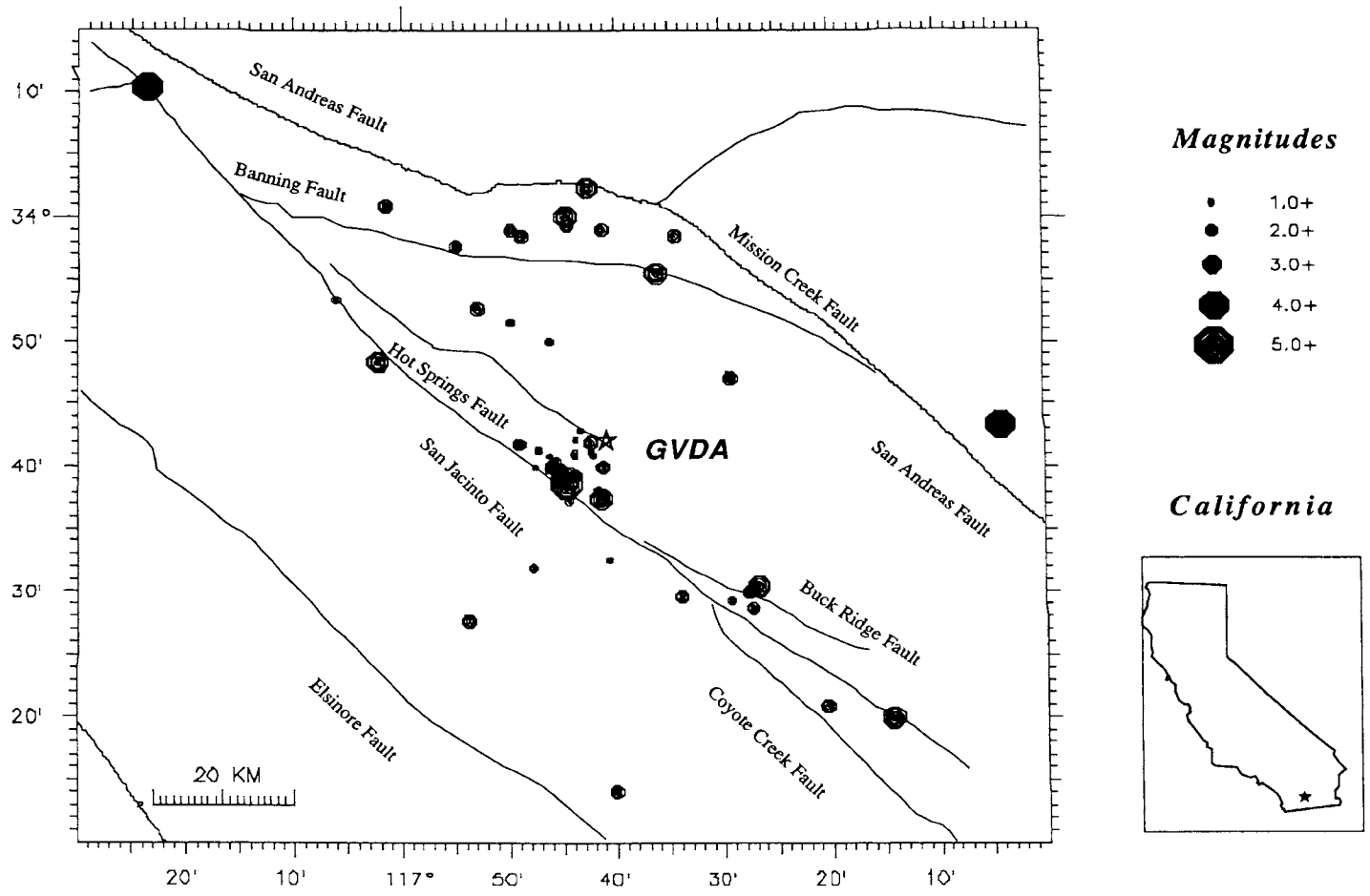


Figure 5. Earthquakes recorded by GVDA from July through December 1989. Note the cluster of events that occurred in December - 9 km from the site. The largest of these was the M 4.2 event of 2 December 1989.

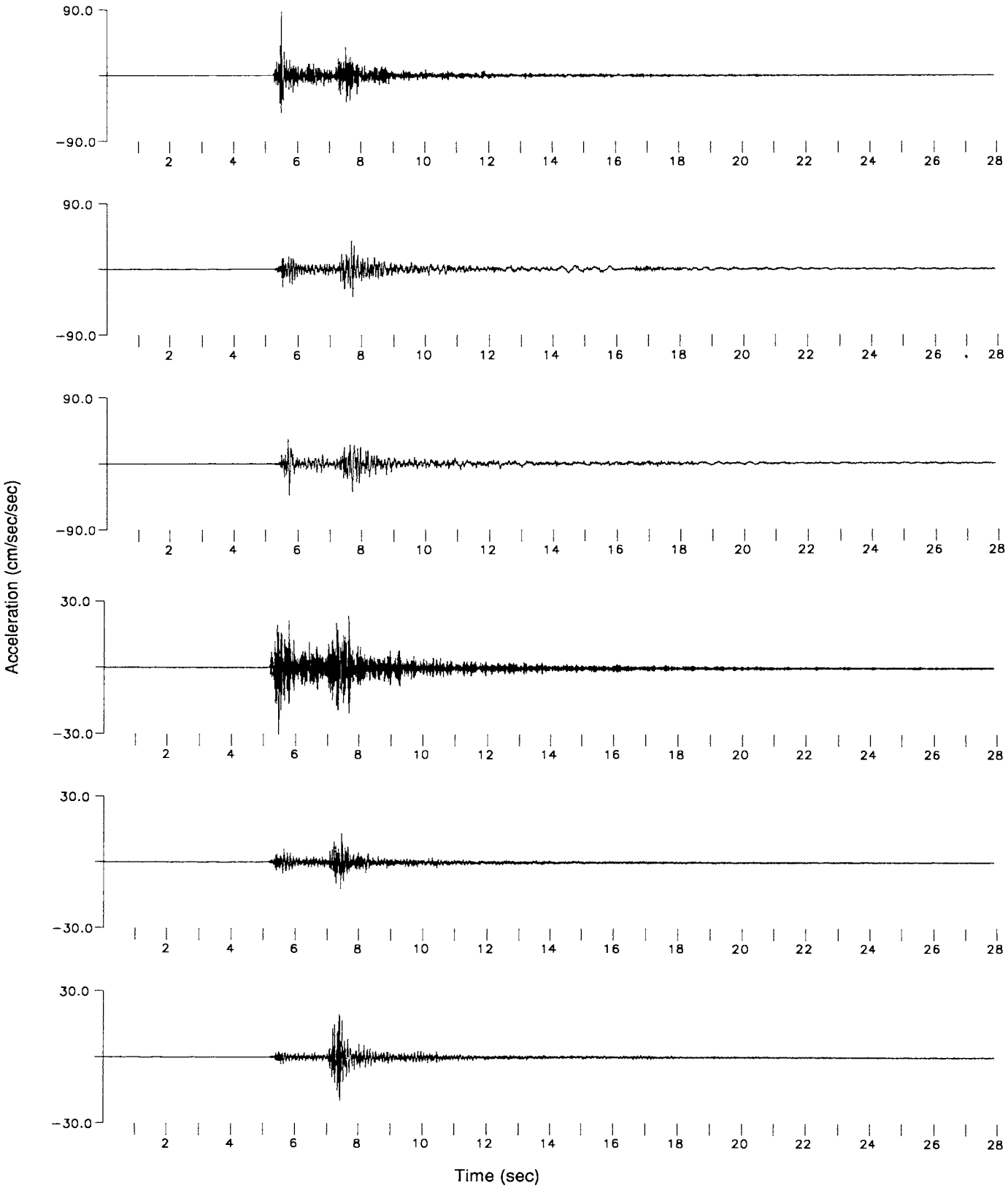


Figure 6. Acceleration records from the 2 December 1989 M 4.2 event. The components are arranged with the vertical component at the top and the two horizontals beneath. a. Accelerations at 0 m. Peak acceleration is 87.6 cm/sec$^2$ on the vertical component. b. Accelerations at 220 m. Peak acceleration is 30.2 cm/sec$^2$ on the vertical component.

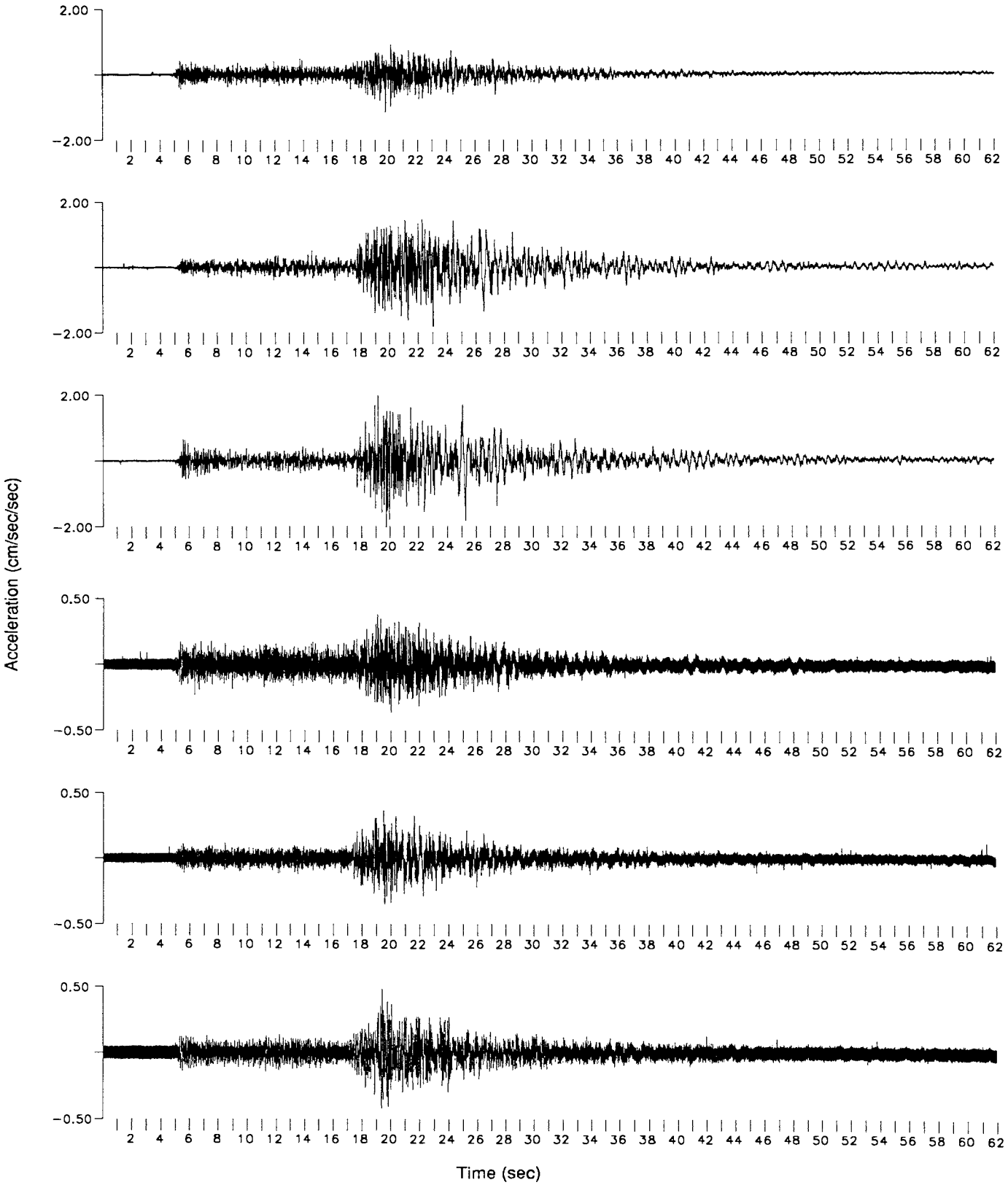


Figure 7. Acceleration records from the 1 March 1990 M 4.7 event. The components are arranged as in Figure 6. a. Accelerations at 0 m. Peak acceleration is 2.048 cm/sec$^2$ on the bottom trace. b. Accelerations at 220 m. Peak acceleration is 0.482 cm/sec$^2$ on the bottom trace.

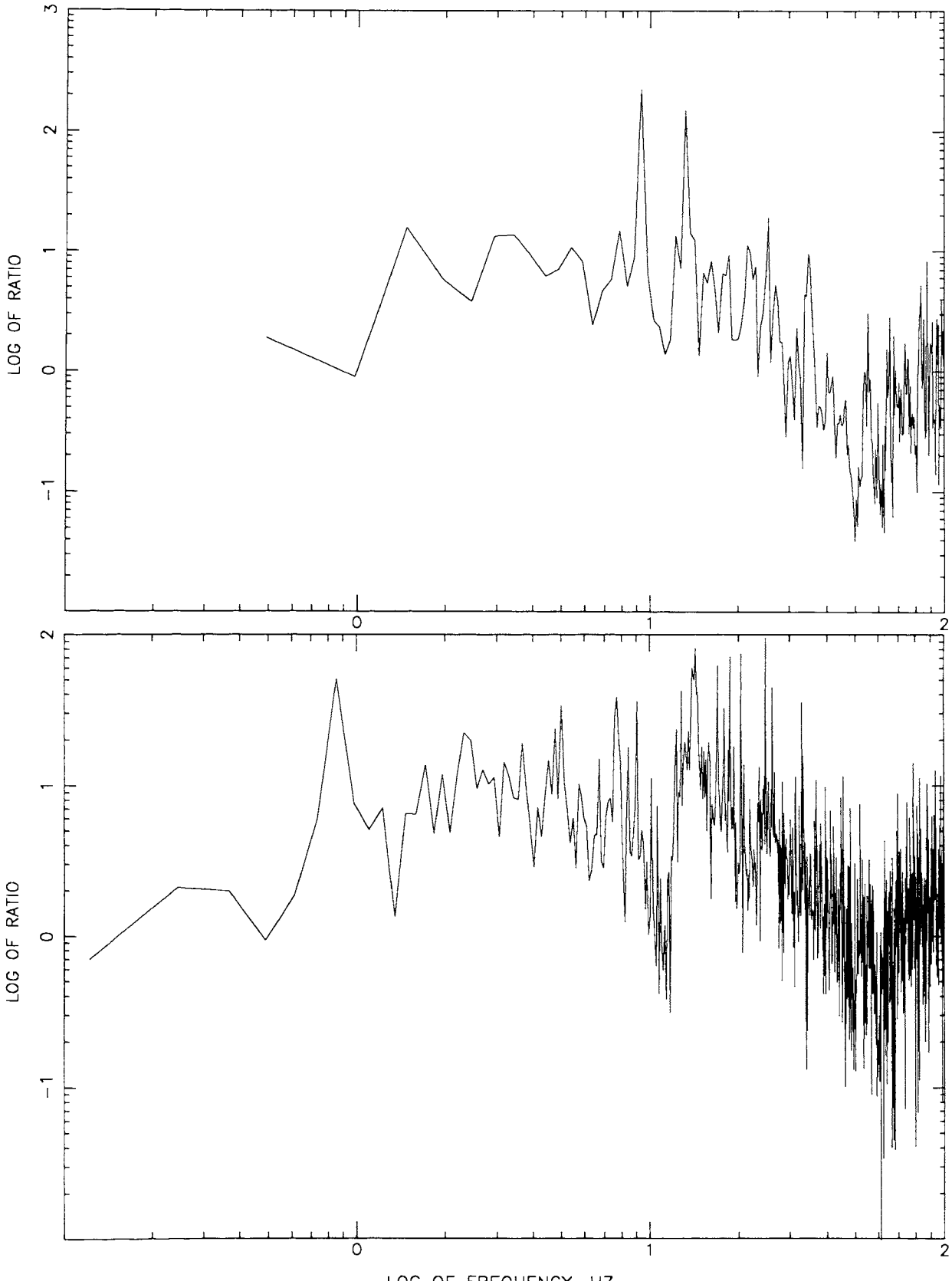


Figure 8. Spectral ratios of S-wave acceleration amplitudes from 0 m to 220 m. Both records show peaks at 9 and 10.5 Hz. Noise dominates after 50 Hz. a. Event of 2 December 1989. b. Event of 1 March 1990. Note peak at 0.9 Hz.

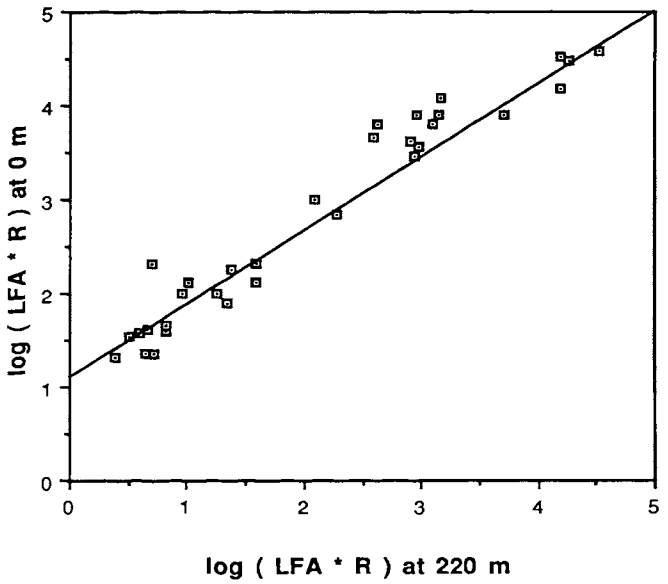


Figure 9. Low frequency asymptote (LFA) x hypocentral distance (R) at 0 m vs 220 m for selected earthquakes. The intercept at LFA x R = 1.0 of the best-fit line (12.8) represents the amplification of the displacements in the lower frequencies (< 5 Hz).

REFERENCES

Archuleta, R. J. and Sangas, P., "Earthquake Source Parameters Determined from the Garner Valley Downhole Array of Accelerometers" (abstract), Seismological Research Letters, 1990, vol. 61, no. 1, 21.

Archuleta, R. J. and Sangas, P., "Preliminary Data and Analysis from the Garner Valley Downhole Array of Accelerometers near the San Jacinto Fault" (abstract), EOS Transactions, American Geophysical Union, 1989, vol. 70, no. 43, 1217-1218.

Archuleta, R. J. and Seale, S. H., "A Cooperative NRC/CEA Research Project on Earthquake Ground Motion on Soil Sites: Data and Preliminary Analysis", Transactions of the 10th International Conference on Structural Mechanics in Reactor Technology, Anaheim, 1989, vol. K1, 85-90.

Brune, J. N., "Tectonic Stress and the Spectra of Seismic Shear Waves from Earthquakes", Journal of Geophysical Research, 1970, vol. 75, 4997-5009.

Fletcher, J., Haar, L., Hanks, T., Baker, L., Vernon, F., Berger, J., and Brune, J., "The Digital Array at Anza, California: Processing and Initial Interpretation of Source Parameters", Journal of Geophysical Research, 1987, vol. 92, no. B1, 369-382.

Gibbs, J.F., "Near-surface P- and S-wave Velocities from Borehole Measurements near Lake Hemet, California", U.S.G.S. Open-File Report 89-630, 1989.

Rockwell, T., Loughman, C., and Merifield, P., "Late Quaternary Rate of Slip Along the San Jacinto Fault Zone near Anza, Southern California", Journal of Geophysical Research, 1990, vol. 95, no. B6, 8593-8605.

Sanders, C. O., "Fault Segmentation and Earthquake Occurrence in the Strike-slip San Jacinto Fault Zone, California", Proceedings of Workshop XLV, Fault Segmentation and Controls of Rupture Initiation and Termination, U.S.G.S. Open-File Report 89-315, 1989, 324-349.

Sangas, P., Archuleta, R. J., and Baker, L. M., "Design, Installation and Digital Recording of a Downhole Seismic Accelerometer Array at Lake Hemet, Ca., near the San Jacinto Fault" (abstract), Seismological Research Letters, 1989, vol. 60, no. 1, 4.

Sykes, L. R. and Nishenko, S. P., "Probabilities of Occurrence Large Plate Rupturing Earthquakes for the San Andreas, San Jacinto, and Imperial Faults, California, 1983-2003", Journal of Geophysical Research, 1984, vol. 89, no. B7, 5905-5927.